GEOPHYSICS, VOL. 78, NO. 5 (SEPTEMBER-OCTOBER 2013); P. J75–J86, 14 FIGS., 2 TABLES.
10.1190/GEO2012-0463.1

An improved and stable downward continuation of potential field data: The truncated Taylor series iterative downward continuation method

HengLei Zhang[1], Dhananjay Ravat[2], and XiangYun Hu[1]

ABSTRACT

We present a stable downward continuation strategy based on combining the ideas of the Taylor series expansion and the iterative downward continuation methods in a single method with better downward continuation and/or computer time/memory performance for potential field data containing noise. In the new truncated Taylor series iterative downward continuation (TTSIDC) method, a correction is made on the continuing plane by downward continuing the difference between the observed and the calculated field. The process is iteratively repeated until the difference meets the convergence conditions. It is tested on synthetic and field data and compared to other downward continuation methods. The proposed method yields sharper images and estimates more accurate amplitudes than most of the existing methods, especially for downward continuation over larger distances. The TTSIDC method also gives comparable results to the method of downward continuation using the least-squares inversion (DCLSI); however, the DCLSI method's requirements of computer memory and time are substantially greater than our TTSIDC method, rendering the DCLSI method impractical for data sets of routine size on desktop computers commonly available today.

INTRODUCTION

Downward continuation is a useful approach to enhance potential fields and their sources, and is used widely in potential fields measured on the ground surface or from airborne and satellite surveys (Langel and Whaler, 1996; Li and Devriese, 2009). A potential field's resolution decreases with increasing observation height. To counter this, downward continuation is applied to estimate the field closer to the source. It also can be applied for source localization at depth (Fedi and Florio, 2011) as in the normalized full gradient method. Unfortunately, the operation of downward continuation is not stable with imperfect or imperfectly approximated data (as with Fourier transforms of finite and discretely sampled data): only after downward continuation by three to five sample intervals, the amplification of high wavenumber noise is so strong that it quickly masks the information in the original data. Some low-pass or smoothing filters can be used for denoising, but experimentation with different high wavenumber cutoffs may be necessary in achieving precise downward continuation.

An optimal downward continuation would provide better resolution and more accurate amplitude, which is necessary for not only qualitative interpretation, but also quantitative calculations. The traditional downward continuation method in the wavenumber domain, i.e., multiplying the downward continuation operator by the Fourier transform of the potential field data and inverse transforming the result, is unstable for reasons discussed above. Pawlowski (1995) proposes a preferential continuation operator using the Wiener filter. The preferential downward continuation can enhance deep sources, but at the expense of removing the high wavenumber anomalies from the data. Recently, several new algorithms have focused on the stability of downward continuation. Fedi and Florio (2002) present a stable algorithm that is based on the computation of stable vertical derivatives obtained by the integrated second vertical derivative (ISVD) method and the Taylor series expansion of the field (called here *integrated second vertical derivative for downward continuation* [ISVDDC]). They apply the ISVD method to obtain stable vertical derivatives to avoid the Taylor series becoming divergent. Trompat et al. (2003) suggest using the ISVD method by removing the edges caused by noise amplification. Cooper (2004) discusses the downward continuation as an inverse problem, and he computes the downward continuation by least-squares inversion (DCLSI) in addition to two other slightly less accurate methods using compensation of ill-effects. Xu et al. (2007) suggest using a type of iteration for downward continuation (called here *iterative downward continuation* [IDC]) that could obtain better results, but

Manuscript received by the Editor 31 October 2012; revised manuscript received 23 April 2013; published online 3 September 2013.
[1]China University of Geosciences, Institute of Geophysics and Geomatics, Wuhan, China. E-mail: sky0610@163.com; xyhu@cug.edu.cn.
[2]University of Kentucky, Earth & Environmental Sciences, Lexington, Kentucky, USA. E-mail: dhananjay.ravat@uky.edu.

they only tested IDC with a noise-free model. For real data containing noise, they tested the method on the data after their upward continuation, but not based on the data observed at higher altitude. Unfortunately, even a small amount of noise is exacerbated in the iteration steps and will lead to a contaminated response. Li and Devriese (2009) discuss the Tikhonov regularization for stable downward continuation (TRDC). They derive an operator for downward continuation by using a regularization parameter in the wavenumber domain. They tested this approach for magnetic data in the unexploded ordnance application with about four sample intervals of downward continuation, which shows it could significantly enhance the anomaly. Recently, the TRDC method was used by Pašteka et al. (2012) for stable downward continuation with a Matlab program which optimally defines the value of the regularization parameter based on C-norm criterion.

Even though the above-mentioned methods improve the stability of downward continuation, most of them do not address the application of the method over large downward continuation distances. We formulate downward continuation as an inverse problem and then an iterative solution is designed for this problem. We show in Appendix A that the iterative strategy is convergent to the theoretical value. We discuss the details of the algorithm, such as the choice of the initial value and the iteration correction. We use model and real data to evaluate not only the stability, but also the accuracy of the algorithm.

THE BACKGROUND

The potential fields on two different planes are related by the solution of the Neumann problem,

$$f(x,y,z) = \frac{z-z_0}{2\pi}\int_{-\infty}^{+\infty}\int_{-\infty}^{+\infty}\frac{f(\varepsilon,\eta,z_0)}{[(x-\varepsilon)^2+(y-\eta)^2+(z-z_0)^2]^{3/2}}\mathrm{d}\varepsilon\mathrm{d}\eta, \quad (1)$$

where $f(x,y,z_0)$ and $f(x,y,z)$ denote the potential field at two observation planes, (x,y) express the horizontal coordinates, and z expresses the elevation. Application of a 2D Fourier transform to equation 1 yields a simpler form in the wavenumber domain,

$$F(u,v,z) = F(u,v,z_0)\cdot e^{-(z-z_0)\cdot 2\pi\sqrt{u^2+v^2}}, \quad (2)$$

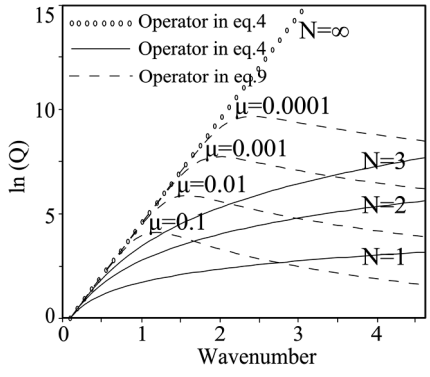

Figure 1. Relationship between wavenumber and amplitude of two downward continuation operators.

where $F(u,v,z)$ and $F(u,v,z_0)$ denote, respectively, the Fourier transform of $f(x,y,z)$ and $f(x,y,z_0)$; $(u,\ v)$ are wavenumbers in the x- and y-directions. When z is greater than z_0, $e^{-(z-z_0)\cdot 2\pi\sqrt{u^2+v^2}}$ is an upward continuation operator and vice versa for a downward continuation operator. It has been shown that for the downward continuation operator, high wavenumbers have high amplitudes, and hence any noise in the data at high wavenumbers is enhanced, rendering the operation numerically unstable. Here, we discuss the key methods developed for controlling amplification of noise at high wavenumbers and then also show examples of their performance.

As an initial strategy, we use thresholding to suppress the amplitudes at high wavenumbers in equation 2 (called here *filtering Fourier transform downward continuation* [FFTDC])

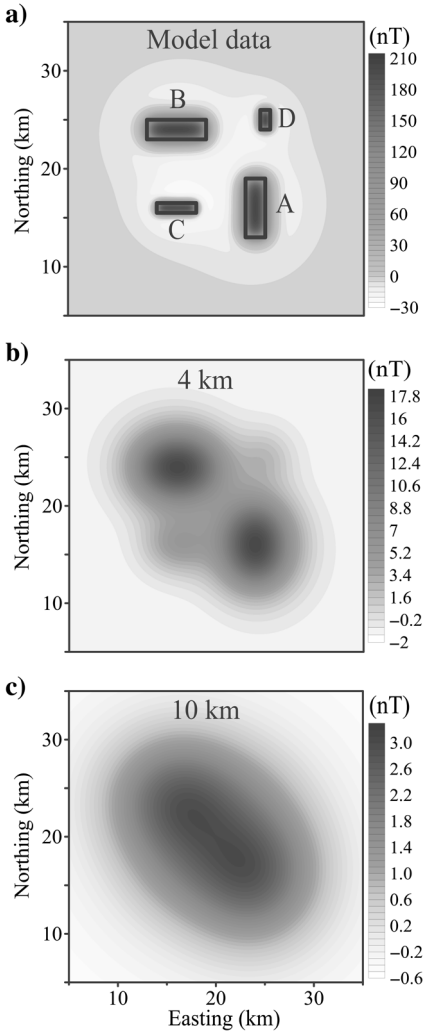

Figure 2. The simulated model data set. The grid interval is 0.2 km. (a) Magnetic response of the synthetic test model. (b) Upward continuation of (a) to a height of 4 km. (c) Upward continuation of (a) to a height of 10 km. To compare with the existing approaches, we will use (b and c) as test data. Model parameters are described in the text.

$$\text{filter} = \begin{cases} 1, & \sqrt{u^2+v^2} \le \text{cof} \cdot M \\ 0, & \sqrt{u^2+v^2} > \text{cof} \cdot M \end{cases}, \tag{3}$$

where M is the maximum of the radial wavenumber $\sqrt{u^2+v^2}$, and cof is the fractional percentage of the maximum radial wavenumber to retain.

The downward continuation operator $e^{2\pi\sqrt{u^2+v^2}\cdot h}$ can be expanded in Taylor series as

$$Q = \sum_{n=0}^{N} \frac{\left[2\pi\sqrt{u^2+v^2}\cdot h\right]^n}{n!}, \tag{4}$$

where h is vertical distance between the original plane and the target plane, and $n!$ is the factorial of n. With the Taylor series approach, to avoid instability due to noise at high wavenumbers, we use the first N terms in the Taylor series expansion as the approximate result. In Figure 1, we show the response function for the Taylor Series downward continuation operator, which indicates that the larger the term N, the greater the amplitude at high wavenumber. To avoid instability, a small N in equation 4 is suitable. Then the downward continuation $f(x,y,h)$ for a potential field $f(x,y,0)$ is calculated as follows

$$f(x,y,h) \asymp FT^{-1}\left[F(u,v,0)\cdot\sum_{n=0}^{N}\frac{\left[2\pi\sqrt{u^2+v^2}\cdot h\right]^n}{n!}\right], \tag{5}$$

where FT^{-1} express the inverse Fourier transform.

The second method we discuss is the ISVDDC of Fedi and Florio (2002) and it is defined as

$$f(x,y,z) = f(x,y,z_0) + \left[\frac{\partial f}{\partial z}\right]_{z_0}\cdot(z-z_0) + \frac{1}{2!}\left[\frac{\partial^2 f}{\partial z^2}\right]_{z_0}\cdot(z-z_0)^2 + \cdots + \frac{1}{(N-1)!}\left[\frac{\partial^{N-1} f}{\partial z^{N-1}}\right]_{z_0}\cdot(z-z_0)^{N-1}. \tag{6}$$

We find that if we transform equation 6 to the wavenumber domain, it will be the same as equation 5. The main strategy of this stable downward continuation approach is to stably compute vertical derivatives from the first order to the Nth-order. Fedi and Florio suggest using Laplace's equation in the computation of the ISVD method to achieve stable vertical derivatives. However, the higher-order derivatives are noisy with their approach. In this paper, we use the Gaussian filter (Gunn, 1999) to compute these derivatives

$$\left.\begin{aligned} f_{xx} &= f \times G_{xx}, \quad \text{where } G_{xx} = \tfrac{x^2-\sigma^2}{\sigma^4}\cdot G \\ f_{yy} &= f \times G_{yy}, \quad \text{where } G_{yy} = \tfrac{y^2-\sigma^2}{\sigma^4}\cdot G \end{aligned}\right\}, \tag{7}$$

where f_{xx} and f_{yy} are the Gaussian-filtered second-order horizontal derivatives and G_{xx} and G_{yy} are the respective Gaussian filter operators. The G_{xx} and G_{yy} are the second derivatives along x-direction and y-direction, respectively, corresponding to the Gaussian function $G = \exp(-\frac{x^2+y^2}{2\cdot\sigma^2})$, where σ is the standard deviation. From the ISVD method with Laplace's equation, any order of vertical derivatives can be computed.

The downward continuation by the least-squares inversion (DCLSI) (Cooper, 2004) is one of the most robust downward continuation methods and it involves the following computation

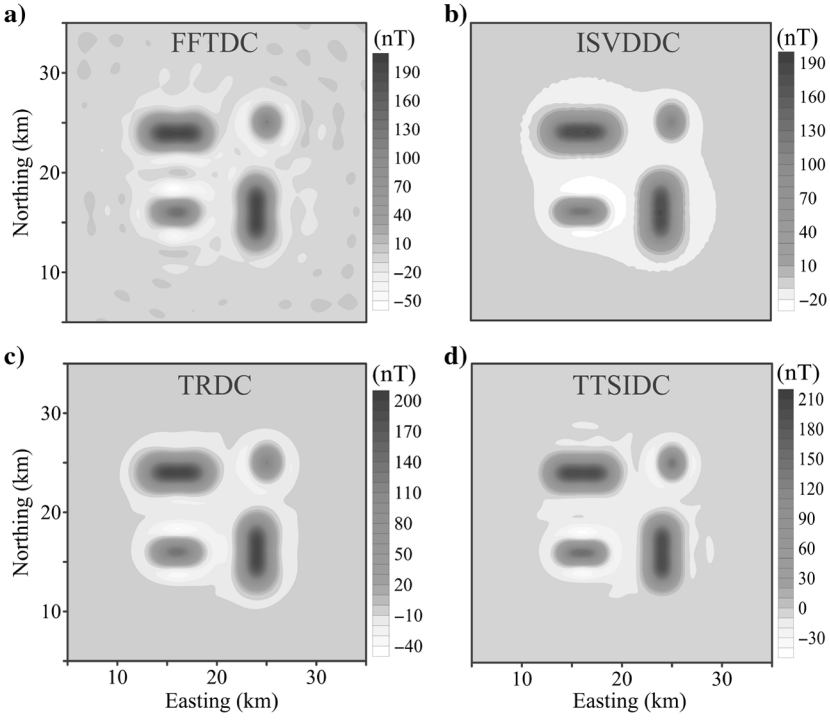

Figure 3. Downward continuations on anomalies in Figure 2b with a vertical distance of 4 km. (a) The result of the FFTDC method with the cutoff coefficient cof = 0.0938 is selected based on Figure 7. (b) The result of the ISVDDC method with the Taylor series expansion terms $N = 11$, and a Gaussian filter is used as shown in equation 7. The optimal value of the standard deviation of the Gaussian filter is 1.0 (based on Figure 8). (c) The result of the TRDC method using the C-norm criterion to optimally define the value of the regularization parameter. This result was computed by Pašteka et al. (2012). (d) The result of the truncated Taylor series interative downward dontinuation (TTSIDC) method proposed in this paper with 250 iterations. We use six terms ($N = 6$) to compute the initial model, and three terms ($N = 3$) to compute the updated models. A Gaussian filter is used as shown in equation 7. The optimal value of the standard deviation of the Gaussian filter is 2.0 (based on Figure 9).

DOI:10.1190/geo2012-0463.1

$$f(x,y,h) = (A^T \cdot A + kI)^{-1} \cdot A^T \cdot e, \tag{8}$$

where A is the gradient matrix, the constant k is a damping factor, I is the identity matrix, and e is the misfit between the original data and the upward continued modified data. This method is, unfortunately, extremely time and memory intensive, as we show later in the paper.

In another method, the IDC (Xu et al., 2007), the initial value on the lower plane is assigned the observed field on plane U: $f_D^0 = f_U$, where f_U is the observed data on plane U, f_D^0 is the initial field on downward continuation plane D. Then, the upward continuation of the initial value f_D^0 on plane D to plane U is calculated. A correction is made for the iteration based on the difference between the original and calculated values on plane U: $f_D^n = f_D^{n-1} + (f_U - f_U^n)$, where f_D^n is the downward continued field after n iterations, f_U^n denotes upward continuation of f_D^{n-1} to original observation plane, repeating the above steps until the corrections become negligible. As described above, we find that if noise is present, it will increase in this method with increasing number of iterations. Another problem in the IDC strategy is that the initial value of the downward continued field is equal to the field observed on a higher plane. Thus, the convergence is always with respect to the initial observed field and not the downward continued field.

Finally, the inverse operator of the Tikhonov regularization downward continuation or the TRDC method (Li and Devriese, 2009; Pašteka et al., 2012) is given by

$$Q = \frac{e^{2\pi\sqrt{u^2+v^2}\cdot h}}{1 + \alpha(u^2+v^2)e^{2\pi\sqrt{u^2+v^2}\cdot h}}, \tag{9}$$

where α denotes regularization parameter. In Figure 1, we show the response function for the TRDC method, which indicates that, the larger the damping parameter α, the smoother the downward continued field, which leads to poorer approximation to the field at lower elevation when it is known in test cases. Pašteka et al. (2012) suggest the use of a C-norm criterion to optimally define the value of the regularization parameter. C-norm (also known as Chebyshev norm or L-∞ norm) is the maximum absolute value of the elements of a vector. The vector, in this case, is the difference between each subsequent iterative solution, which is plotted against the value of the damping or regularization parameter (α). The local minimum of the C-norm function yields the optimum value of α.

THE PROPOSED METHOD

In our study, we combine the Taylor series and the IDC approach above to yield a better-performing method. We also give a proof of convergence of the method in the appendix which has not been given for the IDC method. In the proposed method, the potential field $f(x,y,0)$ observed on the original plane is treated as the data, and the downward continued field $f(x,y,h)$ on the target plane will be treated as the model. With this setup, upward continuation defines a forward mapping and the inverse problem is to seek a well-behaved $f'(x,y,h)$ that reasonably reproduces the data $f'(x,y,0)$ with the smallest difference with respect to the original anomaly, $f(x,y,0)$. The goal is to minimize the root mean square (rms) between them. We define the data misfit function as

$$\text{rms} = \frac{1}{M \cdot N}\sqrt{\sum_{x=1}^{M}\sum_{y=1}^{N}(f(x,y,0) - U_h(f(x,y,h)))^2}, \tag{10}$$

where U_h denotes upward continuation with a vertical height of h, and (M, N) indicates the size of the data. In this study, we use

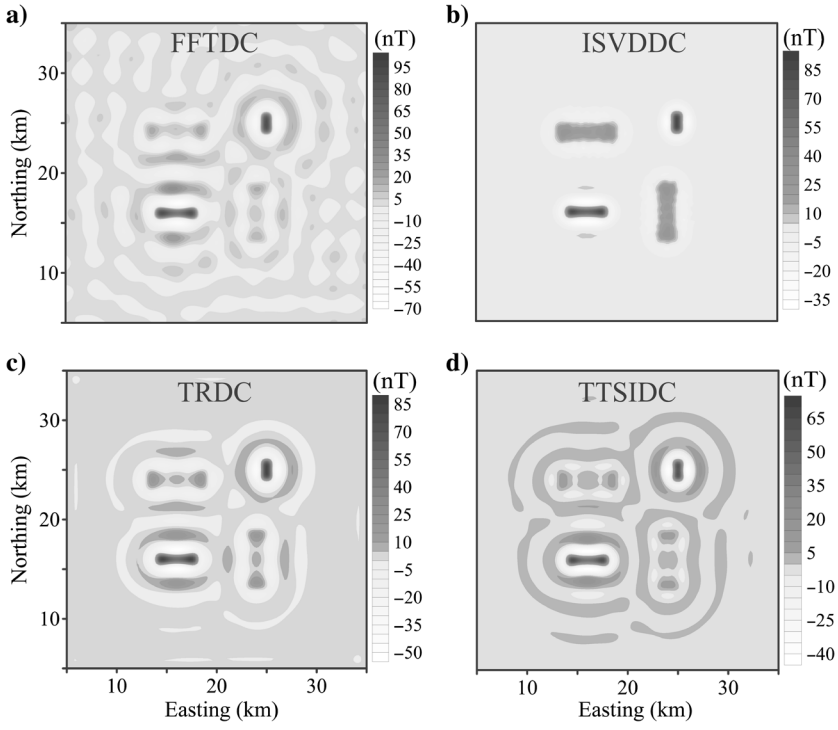

Figure 4. The difference between the theoretical value shown in Figure 2a and the downward-continued results shown in Figure 3.

DOI:10.1190/geo2012-0463.1

the ISVDDC method to compute the initial model. We use D_h^{-1} to denote the downward continuation operator, $f^0(x,y,h) = D_h^{-1}(f(x,y,0))$ indicates the initial model of downward continuation field. Using this premise, an iterative algorithm can be designed as follows:

$$f^i(x,y,h) = f^{i-1}(x,y,h) + \Delta m_i, \tag{11}$$

where Δm_i expresses a model change in each iteration step,

$$\Delta m_i = D_h^{-1}(f(x,y,0) - U_h(f^{i-1}(x,y,h))), \tag{12}$$

where U_h denotes an upward continuation operator with a vertical distance of h, and D_h^{-1} denotes an approximate downward continuation in equation 6 with a vertical distance of h. Thus, we can rewrite the iterative equation 11 as

$$f^i(x,y,h) = f^{i-1}(x,y,h) + D_h^{-1}(f(x,y,0) - U_h(f^{i-1}(x,y,h))). \tag{13}$$

As described above, the calculation of the stable downward continuation algorithm proposed in this paper (called the *truncated Taylor series iterative downward continuation* [TTSIDC]) is as follows:

1) We first compute the initial model $f(x,y,h)$ on the continuing (lower) plane based on the first N terms (where N is shown in equation 6, we set $N = 6$ based on empirical tests) in the Taylor series expansion;
2) Upward continuation of $f^i(x,y,h)$ to $f^i(x,y,0)$, and computation of the data misfit between $f^i(x,y,0)$ and $f(x,y,0)$, where $f^i(x,y,h)$ denotes the potential field on a continued plane after i iterations. If it does not meet the condition set for data misfit, we reiterate the process;
3) The magnitude of the change in the model is based on the consideration of the difference $dt_i = f(x,y,0) - f^i(x,y,0)$ on the plane of original observation. Using the difference, we obtain the model correction as follows: $\Delta m_i = D_h^{-1}(dt_i)$, where N is the number of terms used in equation 6 (we set $N = 3$ based on empirical tests).
4) Adding $f^i(x,y,h)$ and Δm_i gives the new model; we then repeat step 2 until it meets the set condition of convergence.

When there is high wavenumber noise in the data, we use an additional amount of initial upward continuation to reduce that noise. We then use the upward-continued field at its height as the observed field. Therefore, some of the formulas above can be modified as follows:

$$f(x,y,-\Delta h) = FT^{-1}\left(F(u,v,0)\cdot e^{-2\pi\cdot\Delta h\cdot\sqrt{u^2+v^2}}\right), \tag{14}$$

$$f(x,y,h) = D_{h+\Delta h}^{-1}(f(x,y,-\Delta h)), \tag{15}$$

$$\Delta m_i = D_{h+\Delta h}^{-1}(f(x,y,-\Delta h) - U_{h+\Delta h}(f^{i-1}(x,y,h))), \tag{16}$$

and

$$f^i(x,y,h) = f^{i-1}(x,y,h) + D_{h+\Delta h}^{-1}(f(x,y,-\Delta h) - U_{h+\Delta h}(f^{i-1}(x,y,h))). \tag{17}$$

For the proposed TTSIDC method, we need to determine parameters of the low-pass filter, e.g., the number of terms and the

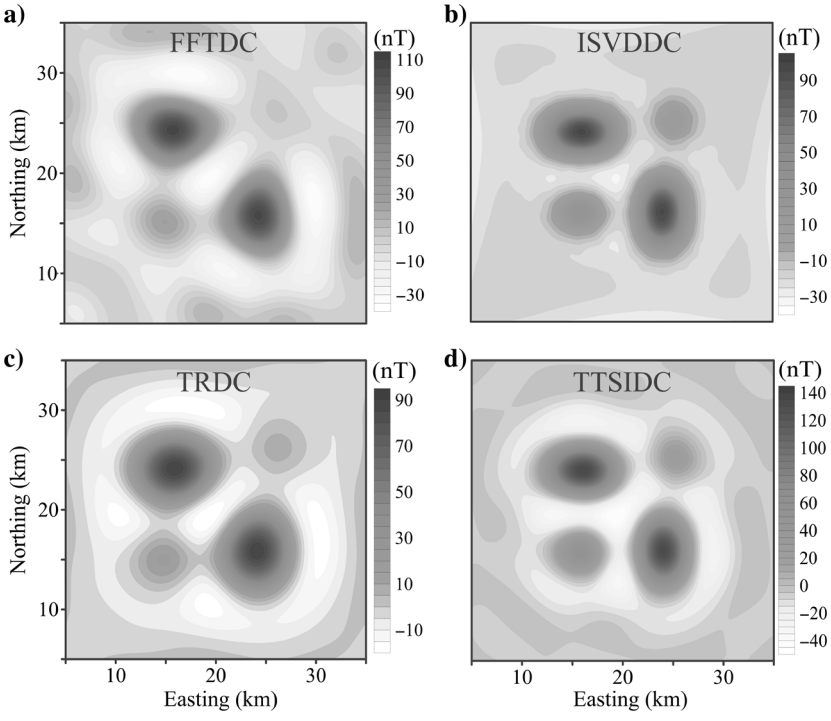

Figure 5. Downward continuations on anomalies in Figure 2c with a vertical distance of 10 km. (a) The result of the FFTDC method with the cutoff coefficient cof = 0.0390 is selected based on Figure 7. (b) The result of the ISVDDC method with the Taylor series expansion terms $N = 11$, and a Gaussian filter is used as shown in equation 7. The optimal value of the standard deviation of the Gaussian filter is 2.0 (based on Figure 8). (c) The result of the TRDC method using the C-norm criterion to optimally define the value of the regularization parameter. This result was computed by Pašteka et al. (2012). (d) The result of the TTSIDC method proposed in this paper with 250 iterations. We use six terms ($N = 6$) to compute the initial model, and three terms ($N = 3$) to compute the updated models. A Gaussian filter is used as shown in equation 7. The optimal value of the standard deviation of the Gaussian filter is 3.0 (based on Figure 9).

DOI:10.1190/geo2012-0463.1

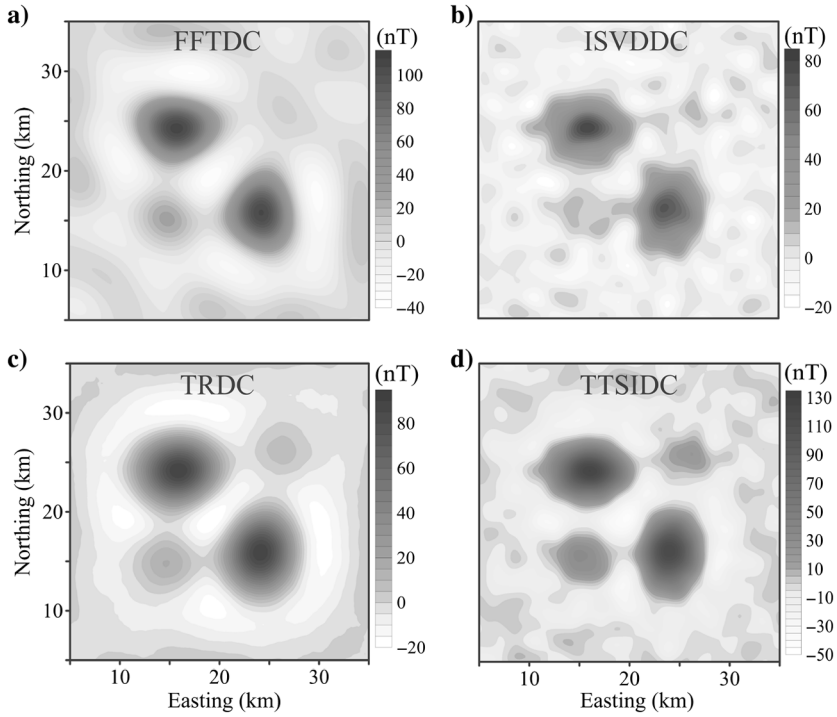

Figure 6. Downward continuations on anomalies in Figure 2c with 1% noise added with a vertical distance of 10 km. (a) The result of the FFTDC method with the cutoff coefficient cof = 0.0390 is selected based on Figure 7. (b) The result of the ISVDDC method with the Taylor series expansion terms $N = 11$, and a Gaussian filter is used as shown in equation 7. The optimal value of the standard deviation of the Gaussian filter is 4.5 (based on Figure 8). (c) The result of the TRDC method using the C-norm criterion to optimally define the value of the regularization parameter. This result was computed by Pašteka et al. (2012). (d) The result of the TTSIDC method proposed in this paper with 250 iterations. We use six terms ($N = 6$) to compute the initial model, and three terms ($N = 3$) to compute the updated models. A Gaussian filter is used as shown in equation 7. The optimal value of the standard deviation of the Gaussian filter is 4.0 (based on Figure 9).

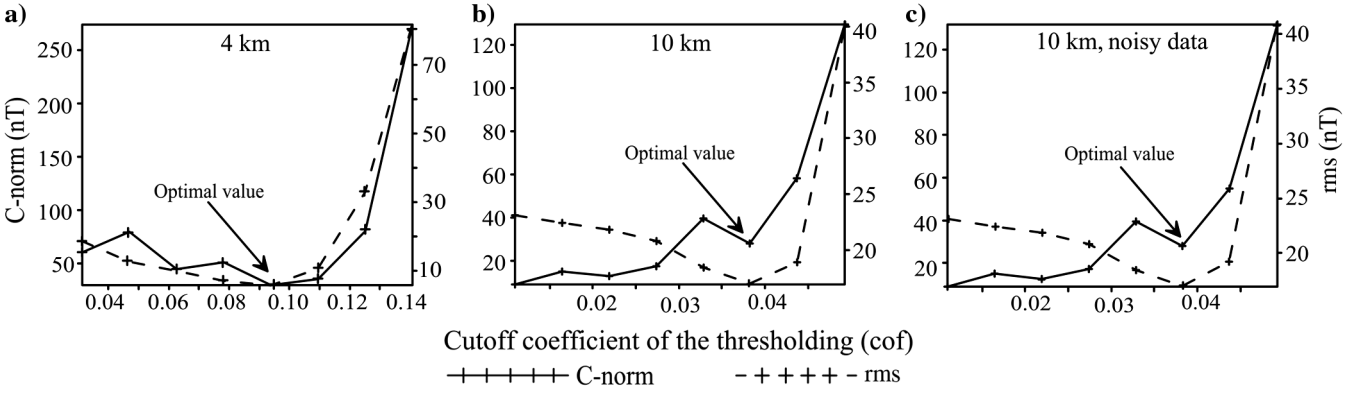

Figure 7. The solid lines show the C-norm for the downward-continued results from the FFTDC method. The dashed lines denote the rms between the downward-continued result and the theoretical anomaly in Figure 2a. The optimal value is at the minimum value and/or the knee of the curves.

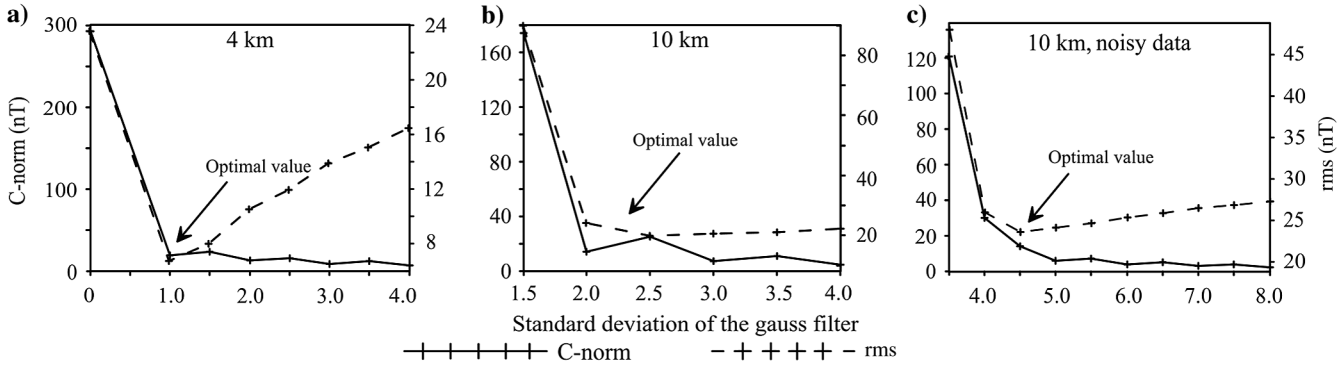

Figure 8. The solid lines show the C-norm for the downward-continued results from the ISVDDC method. The dashed lines denote the rms between the downward-continued result and the theoretical anomaly in Figure 2a. The optimal value is at the minimum value and/or the knee of the curves.

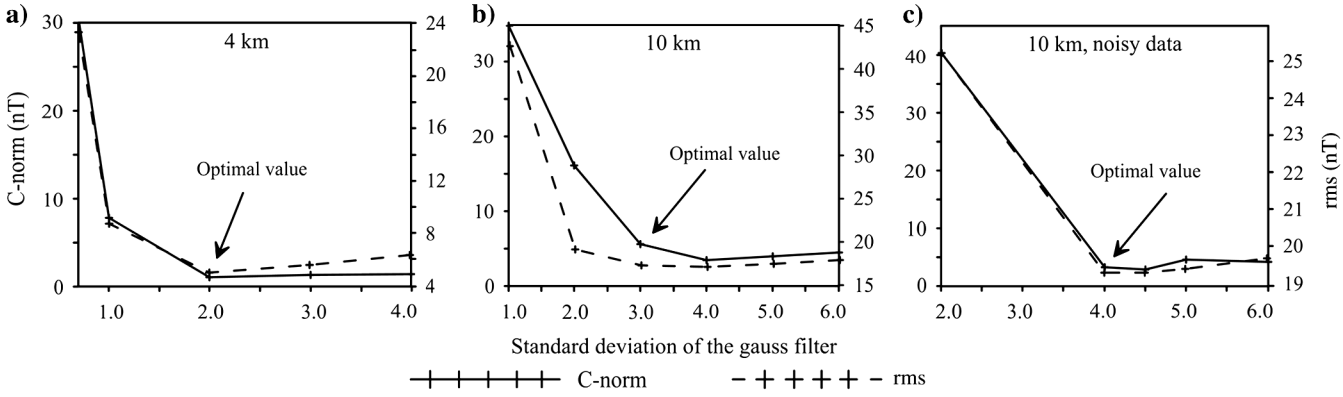

Figure 9. The solid lines show the C-norms for the downward-continued results via the TTSIDC method. The dashed lines denote the rms between the downward-continued result and the theoretical anomaly in Figure 2a. The optimal value is at the minimum value and/or the knee of the curves.

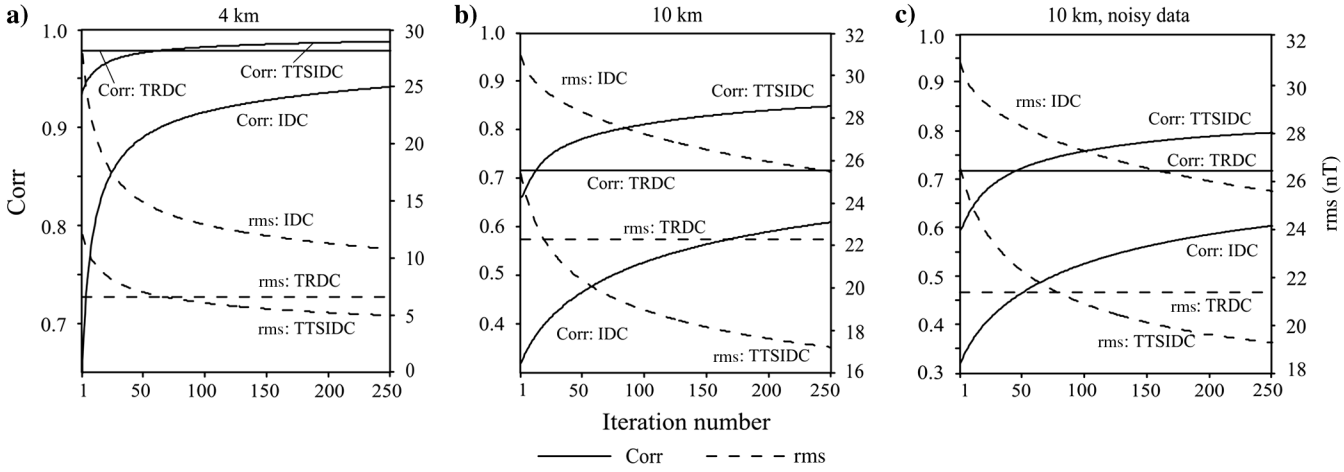

Figure 10. The correlation coefficient (Corr) and rms between the results of downward continuation by different methods and the theoretical value shown in Figure 2a. The solid lines denote the correlation coefficient, and the dashed lines denote the rms. For the TRDC method, we show the Corr and rms between the TRDC results and the theoretical value.

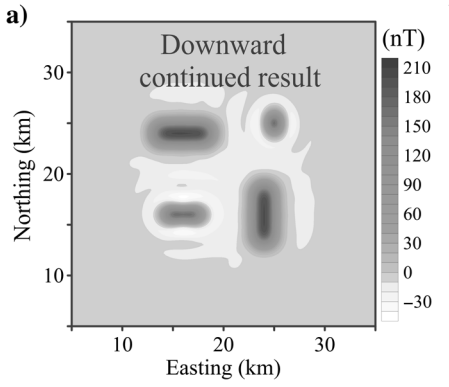

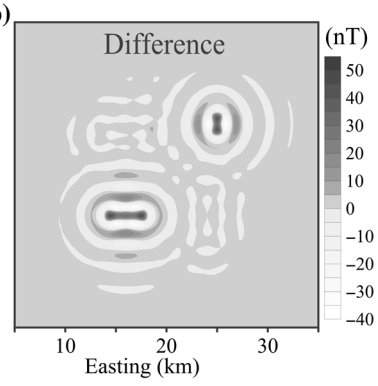

Figure 11. (a) Downward continuation based on the DCLSI method for Figure 2b with a vertical distance of 4 km. The damping factor is 10^{-10}. This result computed on Danish Technological Institute's supercomputer cluster took 76 GB of memory and 120 CPU hours. Compare this result with the TTSIDC result in Figure 3d, which took 5.5 CPU minutes on a 2 GB computer. See the text for details. (b) The difference between the theoretical value shown in Figure 2a and the downward continued result shown in (a).

standard deviation of the Gaussian filter in the Taylor series, the conditions for terminating the iterative process, and the initial upward continuation distance. In principle, the larger the number of terms, the better the downward continued result. In this paper, the Gaussian filter is applied to compute higher-order derivatives. Based on empirical tests with different combinations of terms, we choose the number of terms in the Taylor series as $N = 6$ and $N = 3$ to compute the initial model, and the updated models, respectively. After the number of terms is determined, we use the C-norm (Pašteka et al., 2012) criterion to optimally define the value of the standard deviation of the Gaussian filters. Second, we show that the TTSIDC method converges upon iterations. Presently, we set the iteration number to 250 to terminate the iterative process based on the observed asymptotic convergence for data with noise in Figure 10. Finally, the goal of using an initial additional upward continuation is to reduce high wavenumber noise; how high the continuation level depends on the amount and nature of the noise.

TEST CASE OF MODEL DATA

We use model tests to compare the proposed method TTSIDC with the existing methods such as the FFTDC method, the ISVDDC method (Fedi and Florio, 2002), the IDC method (Xu et al., 2007), and the TRDC method (Pašteka et al., 2012). Computations of the DCLSI method are discussed in the next section. Figure 2a shows the magnetic response from the four vertical-sided prisms (A, B, C, and D whose tops are at depths of 1.0, 1.0, 0.5, and 0.5 km and bottoms are at the depth of 2.0, 2.0, 1.0, and 1.0 km, respectively). The edge locations are indicated by the black lines. All of the prisms have the same magnetization contrast of 1.0 A/m. The inducing field has an inclination of 90° and a declination of 0°. The computed model anomaly at 0.2 spacing is shown in Figure 2a. The beginning and end points of the data are at 0 and 40 km, respectively, in x and y directions. Figure 2b and 2c are upward continuations of the data in Figure 2a by 4 and 10 km, respectively. A perfect downward continuation of Figure 2b and 2c to the original plane should correspond to Figure 2a.

The downward-continued data through the methods FFTDC, ISVDDC, TRDC, and TTSIDC are shown in Figures 3, 5, and 6. We use the C-norm criterion to define the value of cof in the threshold for the FFTDC method, and the value of the standard deviation of the Gaussian filter for the ISVDDC method as well as the TTSIDC method. As shown in Figures 7, 8, and 9, the optimal values are picked at the minimum value and/or the knee of the C-norm curves; such picks are also consistent with therms estimate. In each of the methods above, the method and the optimum amount of smoothing required to stabilize the downward continuation are different. Therefore, we have used objective approaches (picks at

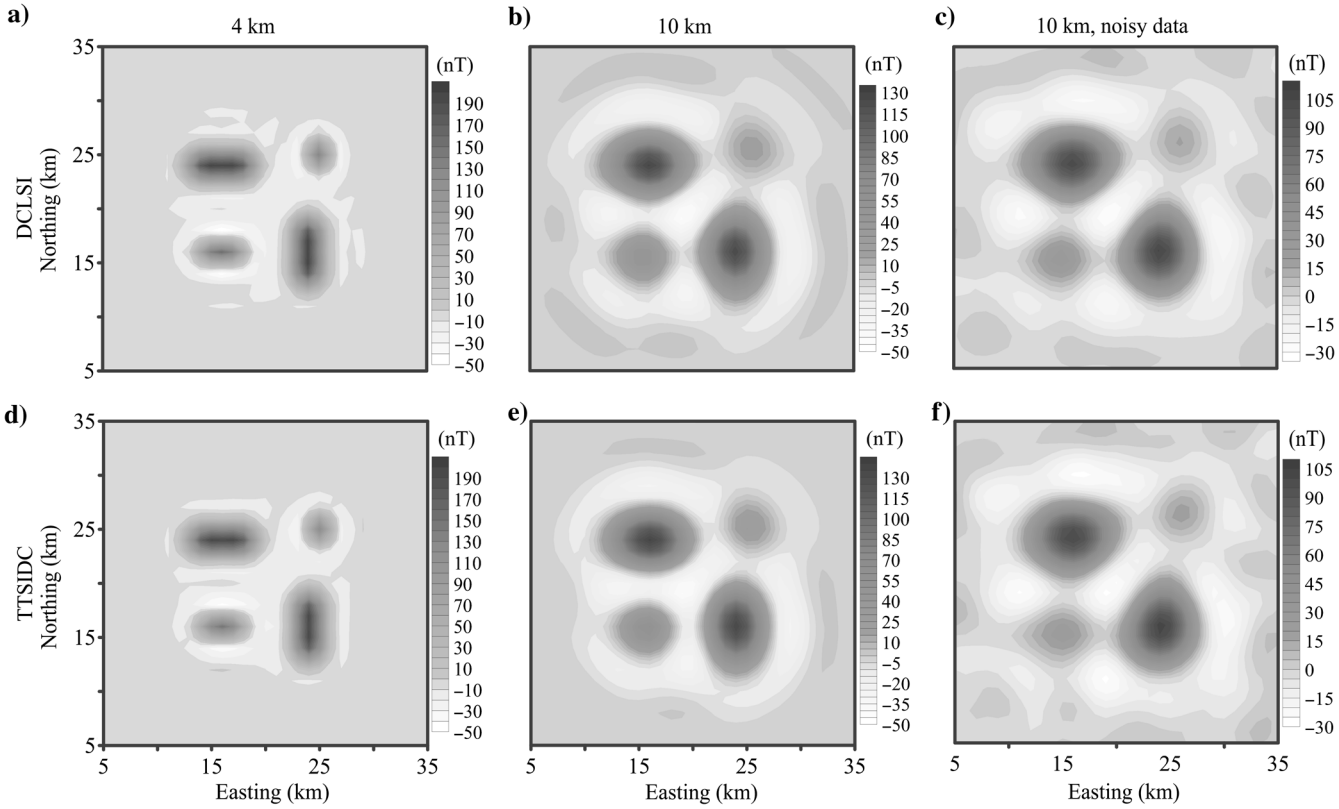

Figure 12. Downward continuation based on the DCLSI and TTSIDC methods for 1 km interval data. For the DCLSI method, the damping factors are 10^{-8}, 10^{-8}, and 10^{-7} corresponding to (a, b, and c), respectively. For the TTSIDC method (shown in d, e, and f), we use 250 iterations to terminate the iterative process. We use six terms ($N = 6$) to compute the initial model, and three terms ($N = 3$) to compute the updated models. For the noisy data, a Gaussian filter with standard deviation of 2.0 is used in this case. We also apply upward continuation of one sample interval distance to avoid high-wavenumber noise contamination.

the minimum values, knees of the curves, etc.) to choose the optimum parameters to compare the methods; these are the objective approaches used by the users of those methods. We discuss here key advantages and limitations of these different methods. First, for downward continuation with a vertical distance of 4 km as shown in Figure 3, most of the methods lead to acceptable anomaly fields, but the amplitudes (minimum and maximum values) of TTSIDC are more similar to Figure 2a. Second, when the downward continuation distance is large (i.e., 10 km as shown in Figure 5), we note that the FFTDC and TRDC methods which use amplitude attenuation in the wavenumber domain produce larger change in the anomaly shapes (features A and B on Figure 2a). Also, the amplitude reduction in the FFTDC, ISVDDC, and TRDC methods is more severe than the TTSIDC method (see Figures 3, 4, and 5, and note that the color scales are different). Besides, at the larger downward continuation distance (Figure 5), the FFTDC and TRDC methods attenuated the amplitude of feature D to the point that it is imperceptible. Moreover, a comparison of downward continuation with noisy data (Figure 6) shows that the ISVDDC method is more susceptible to noise and the anomalies of C and D cannot be distinguished from the noise. Besides, comparison of the differences (shown in Figure 4) between the theoretical value (Figure 2a) and the downward-continued results from all of the methods (Figure 3), the amplitudes (minimum and maximum values) of TTSIDC are smallest. In general, the accuracy of continuation decreases as the continuation distance increases. For the TTSIDC method, this is expected because it uses the truncated Taylor series for stable downward continuation. Despite these shortcomings, it is clear that the TTSIDC method yields more accurate results than the other methods.

In Figure 10, we use correlation coefficient (Corr) and rms as measures to compare the results of the TTSIDC, IDC, and TRDC methods. We can see that the TTSIDC and TRDC methods perform better than the IDC method, and the TTSIDC method obtains the highest Corr and lowest rms with respect to the theoretical value. For downward continuation over the distances of 10 km (50 times the data spacing), it is clear that the TTSIDC method performs better than the TRDC method.

COMPARISON WITH THE DCLSI METHOD

Cooper (2004) presents three methods of downward continuation, of which the DCLSI is the most accurate. However, he pointed out that the DCLSI method is slow and needs large memory because the downward continuation of an N point data set requires the inversion of an $N \times N$ matrix. For a map data of the test example in Figure 2 with 201×201 points, the scale of the matrix is $2012^2 \times 201^2$, which, considering other intermediate matrices, needed 76 GB memory and 120 CPU hours (about four clock hours) on Danish Technological Institute's 8 quad-core AMD Opteron 8356 CPUs with a total of 128 GB RAM, each running at 2.3 GHz. By comparison the TTSIDC method takes only 5.5 CPU minutes for this example on a laptop with two cores. The comparison of the two results is shown in Figure 11, the misfit of the DCLSI result shown in Figure 11b is similar to the misfit of the TTSIDC result shown in Figure 4d. The correlation coefficient (the degree of association), slope (amplitude ratio), and intercept

Table 1. The computation time for the TTSIDC method and the DCLSI method on the decimated data. In the text, we show that for a 201×201 data set at 0.2 km spacing, the DCLSI method is impractical for routinely available computers today.

	4 km data (1 km interval)	10 km data (1 km interval)	10 km data with noise (1 km interval)
DCLSI method	34.97 s	35.05 s	35.61 s
TTSIDC method	10.49 s	10.53 s	32.08 s (The Gaussian filter used at each iteration leads to longer computation time in this case.)

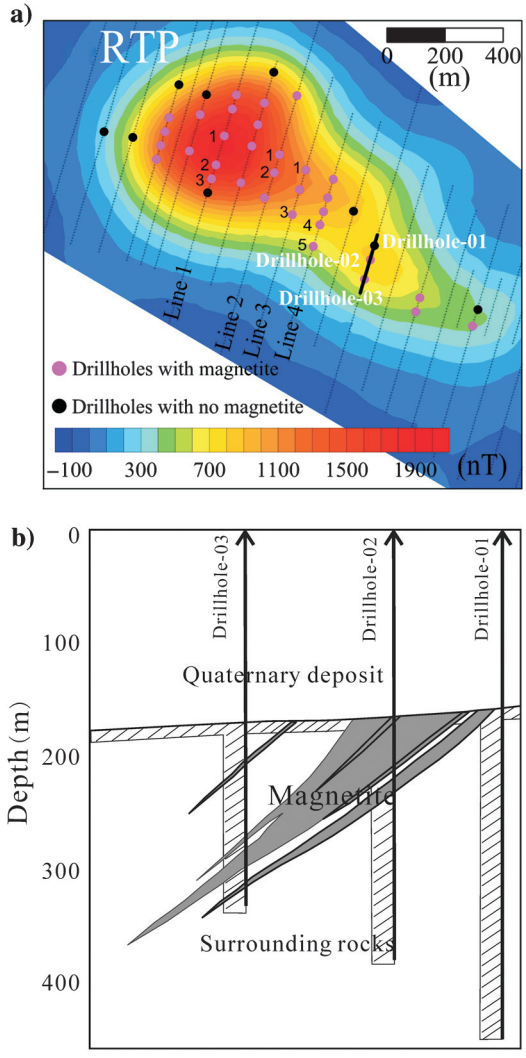

Figure 13. (a) Reduced-to-pole magnetic data over a mine in northwest China's Qinghai Province. The grid interval is 5 m and the total number of the actual data points in the grid is 213,565. Observations are along thin solid black lines, with the line spacing of 50 to 100 m. (b) A cross section of the known magnetite ore body intersected by drillholes (vertical black arrow lines). Magnetite deposits are mainly located below the depth of 150 m. The cross section location is indicated by the solid black line shown in (a) from drillhole-03 to drillhole-01.

(base-level difference) between the model data and the DCSLI method are CC = 0.9940, Slope = 0.9850, and intercept = −0.5650 nT, whereas between the model data and the TTSIDC method, they are very close to the DCSLI method: CC = 0.9877, Slope = 0.9665, and intercept = 0.3371 nT. Because it is not possible to compute the model data on routinely available desktop computers, we decimated the model data to 1 km interval for further comparisons between the DCLSI and our proposed TTSIDC method. The results are similar (shown in Figure 12). Also, as shown in Table 1, the DCLSI method needs much more time than the TTSIDC method. From the 201 × 201 example discussed before, it is clear that for routinely used large data sets in the potential field applications today, the DCLSI method is not practical. On the other hand, the TTSIDC method yields results similar to this method in a very short amount of time and therefore it is feasible on routinely available desktop or laptop computers today.

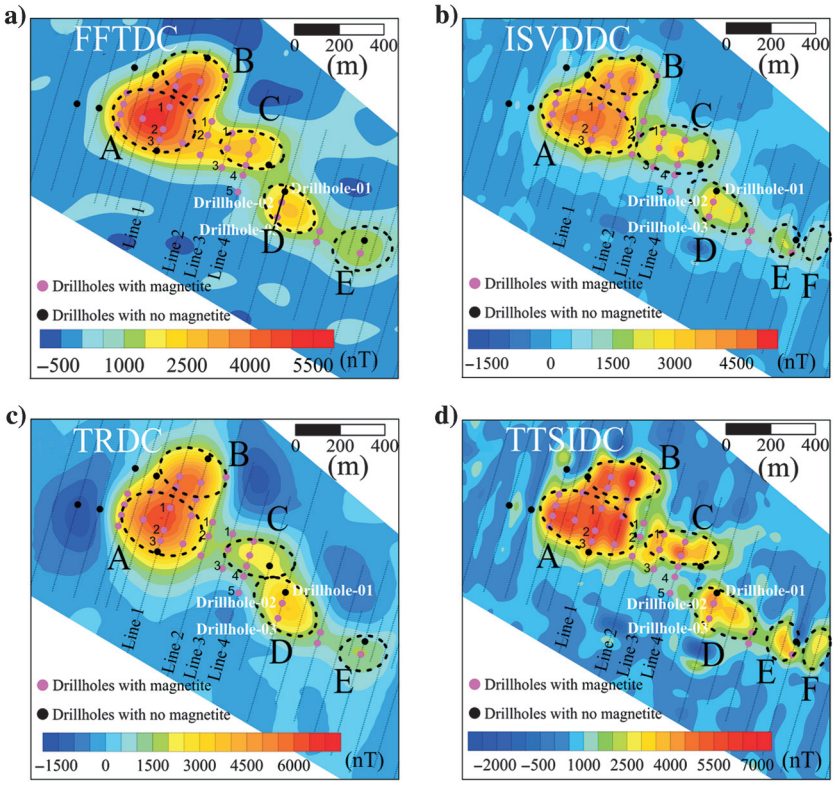

Figure 14. Downward continuation of the RTP data in Figure 13a with a vertical distance of 150 m. (a) The FFTDC method with the cutoff coefficient cof = 0.025. (b) The ISVDDC method with the Taylor series expansion terms $N = 11$, and the standard deviation of the Gaussian filter $\sigma = 6.0$. (c) The TRDC method using the C-norm criterion to optimally define the value of the regularization parameter. This result was computed by Pašteka et al. (2012). (d) The TTSIDC method with 50 iterations, and the standard deviation of the Gaussian filter $\sigma = 5.0$. We use six terms ($N = 6$) to compute the initial model, and three terms ($N = 3$) to compute the updated models. For avoiding contamination from noise, we apply upward continuation of 10 sample intervals (i.e., upward continuation by 50 m) and the modified approach of equations 14–17.

APPLICATION TO A FIELD CASE

The case study is of the exploration of magnetite ore bodies and the area is located in the Qinghai Province region of Northwest China. In this area, the magnetite ore has a very high magnetic susceptibility (6.296 SI), whereas other rocks have much weaker susceptibility (0.005–0.013 SI) (Zhu et al., 2011). Hence, magnetic anomalies are caused mainly by magnetite. Figure 13a shows the reduced-to-pole total field anomaly, and Figure 13b shows a depth section based on drilling information; the magnetite ore is mainly located below the depth of 150 m (Figure 13b). Because of the relatively large depth of magnetite in comparison to the size of the anomaly feature, only one broad elongated anomaly is seen in Figure 13a. It would be desirable to resolve individual magnetite ore bodies for planning the mining operations.

Figure 14 shows the results of downward continuation of the anomaly in Figure 13a by a vertical distance of 150 m below the ground surface from four methods. The selected parameters for each of the method are defined based on the C-norm criterion. Among the four results, the FFTDC and the TRDC, which use amplitude thresholding of wavenumbers, are the smoothest. The amplitudes of the FFTDC and the ISVDDC methods shown in Figure 14a and 14b are significantly lower than the TRDC (Figure 14c) and the TTSIDC (Figure 14d) methods (and hence cannot be meaningfully plotted with the same color scale). The results show that all of the methods improve the resolution of the likely locations of the ore bodies. Although we do not have a bedrock geologic map because of the thick Quaternary overburden, these methods reveal a clearer relationship between magnetite-bearing and nonmagnetite-bearing drillholes and the downward continued anomaly. Below, we discuss the specific details of the relationship.

Table 2. The depth and the total thickness of the magnetite ore in the drillholes in the case study area. The drillholes located on Lines 2 and 4 show that the magnetite ore there is deep and the thickness of the magnetite ore body is thin, but variable depending on the location of the drillhole. The line number and the drillhole number are shown on Figures 13a and 14.

Line number	Line 1			Line 2		Line 3		Line 4	
Drillhole number	1	2	3	1	2	1	3	4	5
Depth of the magnetite ore	349 m	210 m	224 m	445 m	236 m	242 m	313 m	314 m	435 m
Total thickness of the magnetite ore	87 m	62 m	35 m	4 m	16 m	30 m	56 m	35 m	1 m

DOI:10.1190/geo2012-0463.1

First, all the methods show the separation between areas A and C, which corresponds to the drillholes shown in Table 2 that the depth of the magnetite ore there is deep and the thickness of the magnetite ore body is thin. Second, all of the methods show that drillholes 4 and 5 on Line 4 (marked on Figures 13 and 14) are not located on the main anomaly (area C) of the continued field. In addition, we note that the ISVDDC and the TTSIDC methods are able to resolve features better than the other two methods. For example, area F is visible on both the maps; however, the TTSIDC result shows area F more clearly. The drillhole with no magnetite located between areas E and F falls on a local minimum of the downward-continued field in Figure 14b and 14d, and thus, resolves the two areas well.

The TTSIDC field has the highest amplitudes for many of the features and also appears to have a better intrafeature resolution (although the latter could, in principle, be noise). When the line spacing is much larger than the observation interval, it can produce some elongated features along the line direction as shown in Figure 14d. Combining these observations with the results of the model study of the effectiveness of different downward continuation methods, it appears that the TTSIDC method's results are better and perhaps more interesting from the point of view of information necessary for the planning of the mining operations.

CONCLUSIONS

We have developed a new stable downward-continuation method for potential field data to estimate the field closer to its sources (in a source free region). Our method uses iterations based on the truncated Taylor series to improve downward continuation. Model tests and the application to the real magnetic data for mineral exploration demonstrate that the TTSIDC method can estimate the field close to the source without enhancing noise and provide images with better spatial resolution and more precise amplitudes. Especially when considering downward continuation involving large distances, the proposed algorithm yields more accurate and detailed field than the existing methods and it is computationally feasible on commonly available computers today. In the case study with real data, the method also yields a much improved picture of the locations of buried magnetite ore bodies in Qinghai Province of China and shows its utility for the interpretation of geology.

ACKNOWLEDGMENTS

H. Zhang thanks University of Kentucky and São Paulo University for making possible his research visits. We thank Roman Pašteka for his help in performing calculations with the TRDC method by means of his program. We also thank Gordon Cooper for useful discussions as well as his kind help with his software. Many thanks go to Alan Reid, an anonymous reviewer, and the Associate Editor for their detailed suggestions and valuable comments. We also thank the Editor and Assistant Editor for their suggestions. The 201×201 test example was run on Danish Technological Institute's supercomputer cluster; we are grateful to Nils Olsen and Lars Tøffner-Clausen for running it for us and providing benchmarking information on the run. This work was in part financially supported by China Postdoctoral Science Foundation (2011M501257), Geological exploration project (12120113101800), Hubei Provincial Natural Science Foundation, China (No. 2011CDA123), and the Fundamental Research Funds for the Central Universities, China University of Geosciences (Wuhan) (CUG120815, CUG120501, CUG120116, CUG130103). D. Ravat thanks the U.S. National Science Foundation for partial support through award EAR-1246921.

APPENDIX A

THE PROOF OF CONVERGENCE OF THE DOWNWARD CONTINUATION

A proof of convergence, which is the main result of the stable downward continuation algorithm, is presented here. In an effort to clarify equation 13, we first recall that

$$f^0(x, y, h) = D_h^{-1}(f(x, y, 0)). \tag{A-1}$$

Its Fourier form is

$$F^0(u, v, h) = F(u, v, 0) \cdot \left(\sum_{n=0}^{N} \frac{\left[2\pi\sqrt{u^2 + v^2} \cdot h\right]^n}{n!} \right). \tag{A-2}$$

Second, we can get the Fourier form of equation 13 as

$$\begin{aligned} F^i(u, v, h) &= F^{i-1}(u, v, h) \\ &\quad + \left(F(u, v, 0) - F^{i-1}(u, v, h) \cdot e^{-2\pi h\sqrt{u^2+v^2}} \right) \\ &\quad \cdot \left(\sum_{n=0}^{N} \frac{\left[2\pi\sqrt{u^2 + v^2} \cdot h\right]^n}{n!} \right). \end{aligned} \tag{A-3}$$

Let Q given by

$$Q = \sum_{n=0}^{N} \frac{\left[2\pi\sqrt{u^2 + v^2} \cdot h\right]^n}{n!}.$$

Using Q, equation A-3 can be rewritten as

$$\begin{aligned} F^i(u, v, h) &= F^{i-1}(u, v, h) \\ &\quad + \left(F(u, v, 0) - F^{i-1}(u, v, h) \cdot e^{-2\pi h\sqrt{u^2+v^2}} \right) \cdot Q. \end{aligned} \tag{A-4}$$

Let P be given by $P = I - e^{-2\pi h\sqrt{u^2+v^2}} \cdot Q$, where I denotes unit matrix.

Equation A-4 can be rewritten as

$$F^i(u, v, h) = F(u, v, 0) \cdot Q + F^{i-1}(u, v, h) \cdot P. \tag{A-5}$$

Combining equation A-5 with equation A-2, we can get a series of equations

$$
\begin{aligned}
F^1(u,v,h) &= F(u,v,0)\cdot Q + F^0(u,v,h)\cdot P \\
&= F(u,v,0)\cdot Q + F(u,v,0)\cdot Q\cdot P \\
F^2(u,v,h) &= F(u,v,0)\cdot Q + F^1(u,v,h)\cdot P \\
&= F(u,v,0)\cdot Q + F(u,v,0)\cdot Q\cdot P \\
&\quad + F(u,v,0)\cdot Q\cdot P^2, \text{and so on.}
\end{aligned} \tag{A-6}
$$

After t iterations, we can obtain

$$
\begin{aligned}
F^t(u,v,h) &= F(u,v,0)\cdot Q + F(u,v,0)\cdot Q\cdot P + \\
&\quad F(u,v,0)\cdot Q\cdot P^2 + \cdots + F(u,v,0)\cdot Q\cdot P^t \\
&= F(u,v,0)\cdot e^{2\pi h\sqrt{u^2+v^2}} \\
&\quad \cdot\left[I - \left(I - Q\cdot e^{-2\pi h\sqrt{u^2+v^2}}\right)^{t+1}\right].
\end{aligned} \tag{A-7}
$$

In the limit t tending to infinity, the equation reduces to

$$
\lim_{t\to\infty}\left(F^t(u,v,h)\right) = F(u,v,0)\cdot e^{2\pi h\cdot\sqrt{u^2+v^2}}. \tag{A-8}
$$

Equation A-8 is the theoretical formula for downward continuation in the wavenumber domain.

REFERENCES

Cooper, G. R. J., 2004, The stable downward continuation of potential field data: Exploration Geophysics, **35**, 260–265, doi: 10.1071/EG04260.

Fedi, M., and G. Florio, 2002, A stable downward continuation by using the ISVD method: Geophysical Journal International, **151**, 146–156, doi: 10.1046/j.1365-246X.2002.01767.x.

Fedi, M., and G. Florio, 2011, Normalized downward continuation of potential fields within the quasi-harmonic region: Geophysical Prospecting, **59**, 1087–1100, doi: 10.1111/j.1365-2478.2011.01002.x.

Gunn, S. R., 1999, On the discrete representation of the laplacian of Gaussian: Pattern Recognition, **32**, 1463–1472, doi: 10.1016/S0031-3203(98)00163-0.

Langel, R. A., and K. A. Whaler, 1996, Maps of the magnetic anomaly field at Earth's surface from scalar satellite data: Geophysical Research Letters, **23**, 41–44, doi: 10.1029/95GL03092.

Li, Y. G., and S. Devriese, 2009, Enhancement of magnetic data by stable downward continuation for UXO applications: 79th Annual International Meeting, SEG, Expanded Abstracts, 1464–1468.

Pašteka, R., R. Karcol, D. Kušnirák, and A. Mojzeš, 2012, REGCONT: A MATLAB based program for stable downward continuation of geophysical potential fields using Tikhonov regularization: Computers & Geosciences, **49**, 278–289, doi: 10.1016/j.cageo.2012.06.010.

Pawlowski, R. S., 1995, Preferential continuation for potential-field anomaly enhancement: Geophysics, **60**, 390–398, doi: 10.1190/1.1443775.

Trompat, H., F. Boschetti, and P. Hornby, 2003, Improved downward continuation of potential field data: Exploration Geophysics, **34**, 249–256, doi: 10.1071/EG03249.

Xu, S. Z., J. Y. Yang, C. F. Yang, P. F. Xiao, S. C. Chen, and Z. H. Guo, 2007, The iteration method for downward continuation of a potential field from a horizontal plane: Geophysical Prospecting, **55**, 883–889, doi: 10.1111/j.1365-2478.2007.00634.x.

Zhu, C. J., Z. W. Zhou, T. Y. Liu, and H. L. Zhang, 2011, Application of high precision magnetic survey to prospecting: A case study in the Galinge ore district of Qinghai Province: Geology and Exploration (in Chinese), **47**, 277–283.